#### **CURRENT REVIEW**

# Realizing the Full Potential of Advanced Microscopy Approaches for Interrogating Plant-Microbe Interactions

- <sup>1</sup> Donald Danforth Plant Science Center, Saint Louis, MO 63132, U.S.A.
- <sup>2</sup> Advanced Bioimaging Laboratory, Donald Danforth Plant Science Center, Saint Louis, MO 63132, U.S.A.

Accepted for publication 1 February 2023.

Microscopy has served as a fundamental tool for insight and discovery in plant-microbe interactions for centuries. From classical light and electron microscopy to corresponding specialized methods for sample preparation and cellular contrasting agents, these approaches have become routine components in the toolkit of plant and microbiology scientists alike to visualize, probe and understand the nature of host-microbe relationships. Over the last three decades, three-dimensional perspectives led by the development of electron tomography, and especially, confocal techniques continue to provide remarkable clarity and spatial detail of tissue and cellular phenomena. Confocal and electron microscopy provide novel revelations that are now commonplace in medium and large institutions. However, many other cutting-edge technologies and sample preparation workflows are relatively unexploited yet offer tremendous potential for unprecedented advancement in our understanding of the inner workings of pathogenic, beneficial, and symbiotic plant-microbe interactions. Here, we highlight key applications, benefits, and challenges of contemporary advanced imaging platforms for plant-microbe systems with special emphasis on several recently developed approaches, such as light-sheet, single molecule, super-resolution, and adaptive optics microscopy, as well as ambient and cryo-volume electron microscopy, X-ray microscopy, and cryo-electron tomography. Furthermore, the potential for complementary sample preparation methodologies, such as optical clearing, expansion microscopy, and multiplex imaging, will be reviewed. Our ultimate goal is to stimulate awareness of these powerful cutting-edge technologies

<sup>†</sup>Corresponding author: K. J. Czymmek; KCzymmek@danforthcenter.org

Current address of H. Berg: 880 Diehl Road, Fenton, MO 63026, U.S.A.

Funding: X-ray microscope work was funded through a research collaboration between C. Topp and Sumitomo Chemical Corporation, Valent Bio-Sciences LLC, and the Donald Danforth Plant Science Center. We also acknowledge imaging support from the Advanced Bioimaging Laboratory (RRID:SCR\_018951) at the Danforth Plant Science Center and usage of the ZEISS Elyra 7 Super-Resolution Microscope and the LEO 912AB Energy Filter TEM acquired through National Science Foundation (NSF) Major Research Instrumentation grants (DBI-2018962 and DBI-0116650, respectively).

e-Xtra: Supplementary material is available online.

The author(s) declare no conflict of interest.



Copyright © 2023 The Author(s). This is an open access article distributed under the CC BY 4.0 International license

and facilitate their appropriate application and adoption to solve important and unresolved biological questions in the field.

Keywords: adaptive optics, confocal microscopy, electron tomography, light-sheet microscopy, serial block-face scanning electron microscopy, super-resolution microscopy, synchrotron, X-ray microscopy, X-ray tomography

Since the first observations of microscopic organisms by light microscopy (Leeuwenhoek 1673) and the later discovery of the first virus (tobacco mosaic virus) from plant sap by transmission electron microscopy (TEM) (Kausche et al. 1939), confirmation by microsopy that microbes were causal agents in plant disease has played a critical role as a tool in diagnostics and understanding of plant-microbe interactions. Indeed, macroscopic observations are routinely augmented by one or both the use of classical and modern stains of bulk tissue and histological analysis of sectioned tissues (Bougourd et al. 2000; Soukup and Tylová 2019). New cellular insights were often garnered by even closer examination of these interactions using one or both scanning electron microscopy (SEM) (Kumar et al. 2012; Pathan et al. 2010; Wightman 2022) and TEM (Mims et al. 2002; Weiner et al. 2022), especially when combined with the application of cryogenic preservation (Bourett and Howard 1990; Mendgen et al. 1991). In the 1980s, the adoption of digital imaging and confocal microscopy with vital stains (Hepler and Gunning 1998; Hickey et al. 2004) followed by various genetic and molecular tools, such as genomic sequencing, mutant analysis, and the advent of fluorescent proteins to track microbes and their proteins, led to many rapid advances in understanding beneficial and pathogenic cellular phenomena. But the pace of change in imaging methods and technologies (light, electron, X-ray, probe), especially in the multiscale and three-dimensional (3D) space, continues to accelerate along with the landscape of what is possible for these new tools to aid our understanding of the cellular underpinnings in plant-microbe interactions. While this review will highlight some representative and seminal work now routinely performed to explore the cell biology of plants and various microorganisms, we will place special emphasis on some of the more recent and newly emerging technologies that have significant and unrealized potential to further transform our understanding of relevant cellular functions and plant-microbe interactions.

# Light Microscopy Approaches

Advanced photon-based imaging approaches have contributed a wealth of information in discoveries in plant pathology and beneficial microbial interactions. Arguably, the most conse-

quential and effective technologies are a family of "optical sectioning" platforms that extract in-focus information from the objective focal plane and enable high-contrast, high-resolution 3D perspectives. These include pinhole based strategies that i) reject out-of-focus light, such as confocal (Cardinale and Berg 2015; Czymmek et al. 1994; Hepler and Gunning 1998) and spinning disk microscopy (Henty-Ridilla et al. 2013; Oreopoulos et al. 2014), ii) restrict illumination to a thin plane, as with multiphoton excitation (Bourett et al. 2002; Czymmek et al. 2002, 2007; Mizuta 2021; Mizuta et al. 2015) and light sheet fluorescence microscopy (Keller and Dodt 2012; Ovec'ka et al. 2022), or iii) via computational extraction using deconvolution (Sibarita 2005) and structured illumination microscopy (SIM) (Gustafsson 2000; Wu and Shroff 2018). Together, these approaches, combined with vital probes and genetically encoded fluorescent proteins, have ameliorated several challenges when working with thick, highly autofluorescent, relatively impermeant, and optically scattering plant tissues, allowing deeper tissue imaging with improved clarity to explore interactions in fixed and living tissues. Deep plant tissue imaging can be extended further by the application of clearing techniques in fixed tissues (Kurihara et al. 2015; Pasternak et al. 2015; Ursache et al. 2018; Warner et al. 2014) or other optically compatible infiltration strategies suitable for live cell work (Littlejohn et al. 2010, 2014). In the genomics era, the advent of Nobel Prize winning molecular tools for expression of fluorescent proteins (FPs) (Chalfie et al. 1994) has been particularly transformative as a tool to explore plant-microbe interactions. FPs enable a way to circumvent the probing barriers imposed by plant and microbe cell walls, providing a potent way to label specific components in living cells of either the host, the pathogen, or both (Bloemberg et al. 2000; Rufián et al. 2018), as well as serving as a convenient way to trace microbe progression in plant tissue. While often specific to the benefits of imaging plant structures alone (without a microbial counterpart), we do encourage readers to explore a number of useful focused reviews that readily translate to plant-microbe interactions (Berg and Beachy 2008; Ckurshumova et al. 2011; Wu et al. 2013). However, numerous examples demonstrate these approaches and their value for elucidating microbe and host response in roots and leaves (Bloemberg et al. 2000; Czymmek et al. 2007; Kankanala et al. 2007; Kim et al. 2022; Ovec ka et al. 2022), including the dynamic temporal and spatial distribution of pathogen ramification, virulence factors, elicitors, and effector proteins (Cui et al. 2021; Khang et al. 2010) (Fig. 1). Likewise, beneficial interactions, such as Rhizobium-legume sym-

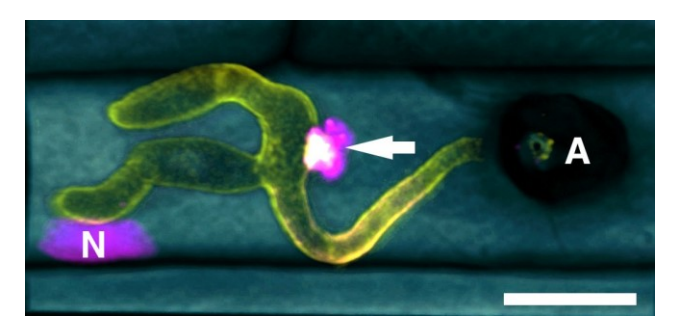


Fig. 1. Live-cell confocal microscopy of fluorescently labeled effectors in plant-pathogen interactions in rice blast disease. *Magnaporthe oryzae* infection of a rice cell showing appressorium (A) and BAS4-GFP-labeled infection hyphae (yellow) and PWL2-mCherry-NLS (magenta) localized in the host nucleus (N), and Calcofluor white–stained cell wall (cyan). A arrow indicates the biotrophic interfacial complex, demonstrating overlapping EGFP and mCherry labeled effector fluorescence signals (Khang et al. 2010). Scale = 10 μm. Image provided courtesy of C. H. Khang (University of Georgia), B. Valent (Kansas State University), and K. Czymmek (Donald Danforth Plant Science Center).

bioses (Chen et al. 2015; Libault et al. 2011; Mendoza-Suárez et al. 2020), arbuscular mycorrhizal (AM) fungi root colonization (Hardham 2012; Ivanov et al. 2019; Martino et al. 2007), and microorganisms that provide protective and growth-stimulating effects (Bloemberg et al. 2000; Jabusch et al. 2021) are ideally suited to optical sectioning approaches. More recently, several fluorescence imaging technologies, termed super-resolution microscopy (SRM), have evolved that break the diffraction optical resolution limit and allow two- to 10-fold better resolution with fluorescent probes than traditional widefield and laserbased imaging (Komis et al. 2015; Schubert 2017; Sydor et al. 2015). One form, SIM, acquires multiple-patterned images to access new frequencies that doubles optical resolution (about 120-nm lateral, 240-nm axial) (Gustafsson 2000). When appropriately coupled with deconvolution, quadruples optical resolution (about 60-nm lateral, 120-nm axial) (Mennella and Liu 2022) allows remarkable visualization of viral protein localization at closely spaced plasmodesmata (PD) pairs, even in living plant cells, not reliably visible with epifluorescence or deconvolution alone (Fig. 2, insets; Supplementary Fig. S1, for PD orientation in the cells). Another SRM approach, single molecule localization microscopy (SMLM), captures a series of thousands of over-sampled images of sparsely spaced single molecules (cre-

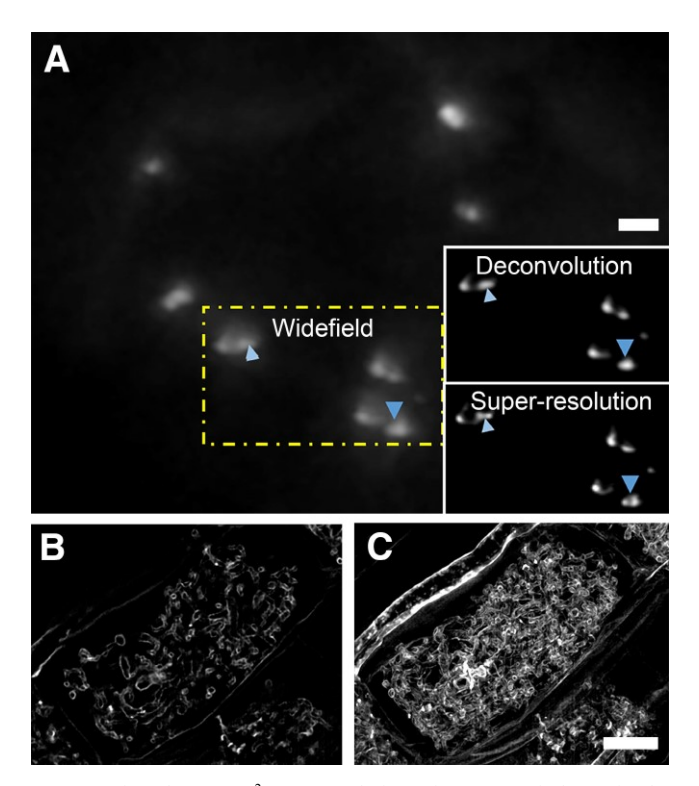


Fig. 2. Zeiss Elyra7 SIM<sup>2</sup> super-resolution microscopy of plant microbe interactions. A, Comparison of imaging approaches and resolution showing tobacco mosaic virus movement protein MP30-GFP localized in plasmodesmata (PD) of Nicotiana benthamiana leaf pitfield, using widefield (yellow dashed box) and corresponding deconvolution and super-resolution (Lattice SIM<sup>2</sup>) image modes (insets). Blue arrows denote the same PD clusters, demonstrating the ability to resolve putative individual paired PD pores compared with widefield and deconvolution. Scale = 1 µm. Image provided courtesy of M. Alazem and T. Burch-Smith (Donald Danforth Plant Science Center). B, Two-dimensional (2D) and C, 3D super-resolution (Lattice SIM<sup>2</sup>) of extensive hyphal branching in cells containing the arbuscular mycorrhizal fungus Rhizophagus irregularis stained with wheat germ agglutinin-Alexa Fluor 488 in Medicago truncatula. Densely branched hyphae were packed within the volume of each inner cortical cell of the root to increase the contact surface for the exchange of nutrients between fungus and plant. Scale = 10 µm. Image provided courtesy of A. Bravo (Donald Danforth Plant Science Center).

ated via blinking or on-off binding effects), finds the centroid of each molecule, and recreates a new image with a 10-fold resolution improvement (Huang et al. 2010). Antibody-based STORM (stochastic optical reconstruction microscopy) (Rust et al. 2006) or genetically encoded fluorescent protein-based PALM (photoactivation localization microscopy) (Betzig et al. 2006) are the most common forms of SMLM and allow flexibility to interrogate subcellular structures depending on probe-type availability (Sydor et al. 2015). While relatively few published reports have demonstrated single molecule or super-resolution microscopy in plant-microbe interactions (Li et al. 2020), a growing number of plant (Komis et al. 2015; Schubert 2017) or microbe (Cattoni et al. 2012; Gahlmann and Moerner 2014; Young et al. 2012) examples illustrate the benefits for resolving targeted nanoscale features. Such improvements in clarity can be appreciated when visualizing the intricate, minute, and closely spaced branching hyphae of symbiotic AM fungi Rhizophagus irregularis within a Medicago root via 3D SIM (Fig. 2B and C).

Another intriguing methodology that uses photon-based imaging, termed expansion microscopy (ExM), is a clever approach that involves infiltrating a specimen with a polymer and anchoring either local proteins, nucleic acids, or both to that polymer, which serves as a uniformly expandable scaffold. The subsequent isotropic expansion of the polymer matrix in an aqueous environment results in a four- to 20-fold increase in sample size (Chang et al. 2017; Chen et al. 2015). Ultimately, ExM provides a way to visualize and interrogate subresolution molecular and cellular features otherwise beyond the diffraction limit, with more routinely available optical and confocal microscopes. While walled plants, microbes, and other organisms present a special challenge for the ExM process (cell walls need to be removed for adequate chemical penetration and expansion), we are encouraged that cell wall enzyme cocktails have been successfully applied in plant and fungal systems (Götz et al. 2020; Kao and Nodine 2021), and we expect mixed organism strategies will be forthcoming.

Improvements in deep and intact 3D/4D plant tissue imaging, thus far, have largely depended on one or more optical sectioning, multiphoton excitation, and clearing techniques. However, leveraging strategies used in astronomy to correct optical distortions as light moves through space, termed adaptive optics (AO), has significant potential to extend further the depth for high-resolution imaging into thick plant tissues. AO uses a reference "guide star"-small fluorescent beads or, in the case of plants, an internal auto- or marker fluorescence—to measure local distortions (cell wall, chloroplast, vacuole) in the optical wavefront caused by sample anomalies. The microscopy system then corrects these errors using a deformable mirror or spatial light modulator (Hampson et al. 2021; Marx 2017). An early application of AO in plants showed that the chloroplast is the single most important structure influencing optical degradation (Tamada et al. 2014). More recently, an advanced implementation of adaptive optics, in combination with lattice light-sheet microscopy, demonstrated the remarkable ability to acquire highspeed, high-resolution 4D volumes with isotropic voxels of bulk samples, including 3D imaging of a green fluorescent protein (GFP) microtubule marker in a live Arabidopsis thaliana cotyledon (Liu et al. 2018). While it is still early days for AO, in light of sample-dependent local optical distortions inherent in multiorganism interactions, we believe it holds much promise not only to visualize problematic deeper tissue interactions but also for 4D dynamic phenomena near the host surface.

## X-Ray Tomography Approaches

X-ray tomography (XRT) imaging, whether done using conventional lab-based instruments or synchrotron beamline sys-

tems, is a powerful method for generating detailed 3D volume data for large and complicated samples that are difficult or impossible to image with other microscopy platforms. In general, XRT generates image data based on variations in sample density, produced by differential attenuation of X-rays as they are passed from the X-ray source through the sample onto a detector. Samples are rotated while hundreds or thousands of digital radiographs are captured, and a 3D volume is computationally generated using a variety of available reconstruction algorithms. X-ray microscopy (XRM) incorporates objective lenses coated with a scintillator that converts X-rays into light, which is magnified by the objective lens before being collected by the detector. Although technical resolution for the various forms of XRT can be calculated, that value is only valid for resolving two high-contrast features (e.g., two tungsten wires), whereas most biological systems cannot achieve such high levels. Scan geometry, sample size and density, X-ray energy, and detector resolution combine to impact the actual biological resolution in any particular situation. For a more thorough treatment of the physics and engineering aspects of XRT imaging, we refer you to an excellent review by Jacobsen (2019).

Although XRT has seen a modest increase in utilization in plant science over the past two decades, relatively little work has been done using XRT to investigate plant-microbe interactions. The main reason for this is that conventional lab-based XRT instruments do not have the resolving power to do sophisticated imaging at the cellular and microbial scale at which plants and microbes interact. In these instruments, magnification is limited by internal cabinet space and the resulting source-sampledetector geometry. On the other hand, lab-based XRM instruments have made more meaningful plant-microbe X-ray imaging possible, as recently demonstrated with soybean root nodules, mycorrhizal fungi, and foliar pathogens (Duncan et al. 2022) and with olive tree cultivars and the bacterial pathogen Xylella fastidiosa (Walker et al. 2023) The majority of XRT research on plant-microbe interactions has used synchrotron beamline systems that allow high-resolution imaging and shorter scan times. Access to synchrotron beam time, however, is often challenging, requiring collaboration, careful communication, and coordination between plant scientists and beamline researchers, reducing the broader adoption of this powerful technology.

There are a number of synchrotron imaging studies in plantmicrobe interactions. For example, synchrotron imaging was applied to explore Esca leaf symptoms in grape leaves to visualize vascular occlusions, embolisms, and evidence of fungal pathogens (Bortolami et al. 2019). Synchrotron XRT was also used to evaluate infection biology in wheat spikes caused by the fungal pathogen Fusarium graminearum, taking advantage of the edge enhancement properties of synchrotron phase contrast imaging (Brar et al. 2019). Synchrotron imaging was also used to examine tomato vasculature for evidence of occlusions caused by the bacterial pathogen Ralstonia pseudosolanacearum (Ingel et al. 2022). Others (Keyes et al. 2022) combined synchrotron XRT with X-ray fluorescence and X-ray absorption near-edge structure elemental mapping to investigate the interaction of wheat roots with the mycorrhizal fungus Rhizophagus irregularis and their spatial relation to phosphorus, sulfur, and aluminum in soil. Hou et al. (2022) addressed the sample-size limitation of some synchrotron systems and demonstrated highresolution imaging of wheat roots in soil cores up to 150 mm in diameter at resolutions of approximately 40 µm, sufficient to evaluate some root-microbe interactions. Synchrotron imaging of leaf mesophyll measured internal surface area (Théroux-Rancourt et al. 2021) and demonstrated imaging resolutions that could be used to visualize foliar pathogens.

Another difficulty in using XRT to study plant-microbe interactions is the typically low contrast of plant and microbial tissues, generating only narrow differences in X-ray attenuation with which to form an image. The use of contrast agents is, therefore, critical for the high-resolution XRT imaging necessary for the microbial scale, whether synchrotron or lab-based. Exogenously applied chemical contrast agents have been tested with regard to improving plant-microbe XRT imaging. Keyes et al. (2017) delivered medical-grade buffered iodine solutions via aerial vasculature to visualize pea plants with a conventional labbased XRT instrument, highlighting xylem and phloem tissues surrounding root nodules. In another example, iodine, bromine, and silver were tested for their ability to enhance soil-plantmicrobe interactions with synchrotron XRT (Lammel et al. 2019). The first significant application of contrast agents to plant samples for lab-based XRM (Staedler et al. 2013) was used in our own research as a starting point for further exploration to include plant-microbe interactions (Duncan et al. 2022). This strategy was applied to an ethanolic phosphotungstic acid-fixed and contrasted root nodule in soybean (Glycine max) colonized by the nitrogen-fixing bacterial species Bradyrhizobium japonicum (Fig. 3). The intact nodule (Fig. 3A; Supplementary Video S1) was rendered in multiscale as a 3D cut-away to reveal overall nodule structures (e.g., arrows are vascular bundles), and the second higher-resolution scan performed (yellow cylinder) revealed individual nodule cells packed with bacteroids, brightly contrasted plant nuclei, as well as uninfected cells (Fig. 3B).

Localization of heavy metals or other high-contrast materials at specific regions of interest is another strategy for enhancing XRT imaging, although we are unaware of any plant biology examples at this time. One early mammalian example (Metscher and Müller 2011) used immune precipitation of metallic silver to selectively label and visualize murine tubulin and collagen with a lab-based XRM. One challenge for adapting heavy metal immunolocalization techniques for XRT in plant-microbe interactions is penetration of the immunological agents through the multiple barriers of plant and fungal cell walls. Geneticallyencoded expression systems are also being used in animal cell research to localize electron-dense compounds for visualization by electron microscopy methods. It may be possible to adapt these to plant systems to allow XRT visualization of microbial interactions. One example is mini singlet oxygen generator, or miniSOG (Ng et al. 2016; Shu et al. 2011), in which a genetically encoded photo-activated protein is expressed that can locally catalyze 3,3-diaminobenzidine (DAB) into an osmiophilic reaction product, readily visualized by electron microscopy. Another is the APEX/APEX2 system in which an ascorbate perox-

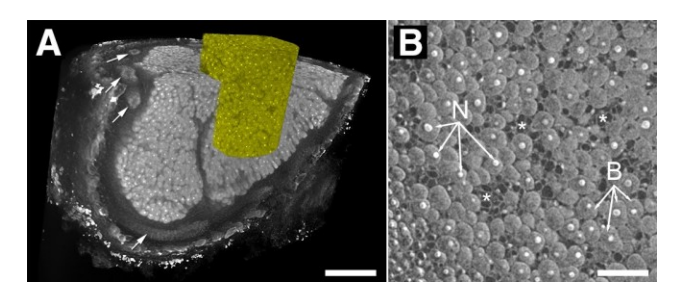


Fig. 3. Multiscale X-ray microscope imaging of soybean nodule. **A,** Three-dimensional (3D) volume rendering (corresponding to Supplementary Video S1) from a multiscale X-ray microscope (XRM) scan of a single root nodule in soybean (*Glycine max*), caused by colonization by the nitrogen-fixing bacterial species *Bradyrhizobium japonicum*. Note the vascular bundles (arrows) that carry nutrients to the nodule and nitrogenous compounds to the host plant. Scale bar = 500 µm. **B,** 2D image slice from a second high-resolution XRM scan from the yellow region of seen in A. Bacteroids (B) are clearly visible, with elevated signal and expanded plant cells with bright plant nuclei (N), as well as uninfected cells (asterisks). Scale bar = 50 µm. Sample prep and imaging methods used were from Duncan et al. (2022).

idase gene is linked to a gene of interest for production of a precipitate upon incubation with DAB and hydrogen peroxide for reaction with osmium (Martell et al. 2017) or silver or gold deposition (Bayguinov et al. 2020; Rae et al. 2021). Finally, others generated fluorescent quantum dots conjugated to a mineral form of phosphorus, e.g., apatite, and used epifluorescence and fluorescence spectral imaging to follow phosphorus uptake by *Rhizophagus irregularis* in an in-vitro carrot root culture system (van't Padje et al. 2021). The use of quantum dots or other electron-dense nanoparticles could be coupled with microbespecific conjugates to locally deposit high contrast material for XRT imaging.

Soft X-ray tomography (SXT) and microscopy (SXM) have recently been used to visualize animal and yeast cells, using cryo-prepared vitrified samples requiring no additional contrast agents, and to generate 3D volume data at the organelle level (Bayguinov et al. 2020; Loconte et al. 2022; Okolo 2022). It is conceivable that, with appropriate cryo-preservation of plant tissues, SXT and SXM could prove valuable additions to the tools available for imaging plant-microbe interactions. There are additional technologies that can complement synchrotron and lab-based XRT imaging of plant-microbe interactions. One example is laser ablation tomography, used to visualize changes in root morphology caused by root-microbe interactions (Strock et al. 2019). Another example is X-ray fluorescence spectroscopy coupled with synchrotron XRT, used to map potassium, calcium, iron, copper, and manganese in wheat leaves infected by the fungal pathogen Pyrenophora tritici-repentis (Naim et al. 2021). Furthermore, positron emission tomography (PET), which can be used to map carbon allocation in roots when <sup>11</sup>CO<sub>2</sub> is delivered to leaves or to map movement of nitrogen into shoots and leaves when <sup>13</sup>N-ammonia is delivered to roots. PET 3D volume data can be coupled with spatial computationally segmented XRT scan data and the two volumes overlaid to map carbon and nitrogen flux relative to root system architecture (Komarov and Tai 2022). These tomography-based analysis tools provide detailed extension to 3D volume data generated with XRT. Finally, we cannot overemphasize the potential power of computational tools, such as DeepRecon, that use deep learning algorithms to denoise 3D volume data from lab-based XRM scans and significantly reduce scan times by generating high-quality 3D volume data with fewer projections (Villarraga-Gómez et al. 2022). Such computational image strategies allow improved resolution, contrast, and visualization as well as more robust segmentation and quantification of relevant features in microbial interactions with their plant host.

## Electron Approaches

Classical TEM and SEM have been primary tools for visualizing microscopic organisms for many decades and, to this day, remain critical to assessing the nature of their interactions. We refer readers to a very useful compendium of various electron microscopy approaches to visualize plant pathogens, including bacteria, mycoplasma, fungi, and viruses (Mendgen and Lesemann 1991). Conventional ambient temperature preparation protocols have established many important findings on plant-microbe interactions, including subcellular chemical immunolocalization (Benhamou and Bélanger 2017) and elemental composition (Eder and Lutz-Meindel 2008). However, depending on the biological question, physical fixation via cryo-preservation remains the gold standard for surface and cytoplasmic ultrastructural studies, when appropriate and possible (Gilkey and Staehelin 1986; Howard 1981; Jeffree and Read 1991; Wightman 2022). This is especially the case with labile or dynamic cellular phenomena and when the special challenges of walled plants and microbes, the plant cuticle, and air spaces impede penetration

of chemical fixatives. For example, high-pressure freezing and freeze-substitution combined with electron tomography (ET) have made possible new discoveries in biology, including examples in plants (Otegui 2020; Weiner et al. 2022), microbes (Hohmann-Marriott et al. 2006) and plant-microbe interactions (Ivanov et al. 2019). ET is an approach in which semi-thick resinembedded sections are incrementally tilted (i.e.,  $\pm 70^{\circ}$ ) and a tomogram is reconstructed to allow fine z-slicing (about 3 nm) and segmentation to produce and visualize high-resolution 3D models of cellular structures. Here, in a deeper dive, we demonstrate the benefits of this approach from two recent studies (Ivanov et al. 2019; Roth et al. 2019) that discovered two membrane systems were produced during arbuscule formation. The fungus produces an extracellular complex of membrane tubules, and the plant host forms a complex of extracellular membrane tubules, the intramatrix compartment (IMC), that permeate the periarbuscular space (PAS) via evagination of the plant-derived periarbuscule membrane. The structure in thin sections of this membrane system (Fig. 4A) appeared to be isolated vesicles, making it imperative to examine this system using 3D ET. Ivanov et al. (2019) used one-micron thick sections and scanning transmission electron microscopy (STEM) tomography, which allows the beam penetration needed for thicker sections, to reveal the 2D (Supplementary Video S2) and 3D structure of the system (Fig. 4B and C; Supplementary Videos S3 and S4). This showed that the tubules have vesicle-sized swellings along their length and that there are few isolated vesicles. Roth et al. (2019) interpreted the plant membrane system to be composed of extracellular vesicles. Perhaps due to under-sampling the z axis (using 250-nm sections) the continuity of the vesicles were not observed. The fungal membrane tubules form by evagination from the fungal protoplast, forming an array (Fig. 4D) that remains attached in places to the fungal protoplast, including maintaining continuity of tubule lumen with protoplast cytoplasm, as clearly shown (Roth et al. 2019). These two systems (fungal tubules and IMC) are well-positioned to facilitate exchange of materials between the symbiotic partners. There have been previous reports of extracellular tubules in mycorrhizal fungi (Bonfante-Fasolo 1987; Cox and Sanders 1974; Dexheimer et al. 1985; Gianinazzi-Pearson et al. 1981) at a time when ultra-rapid cryofixation was not generally available. These studies used chemical fixation and solvent dehydration. Chemical fixation is a slow

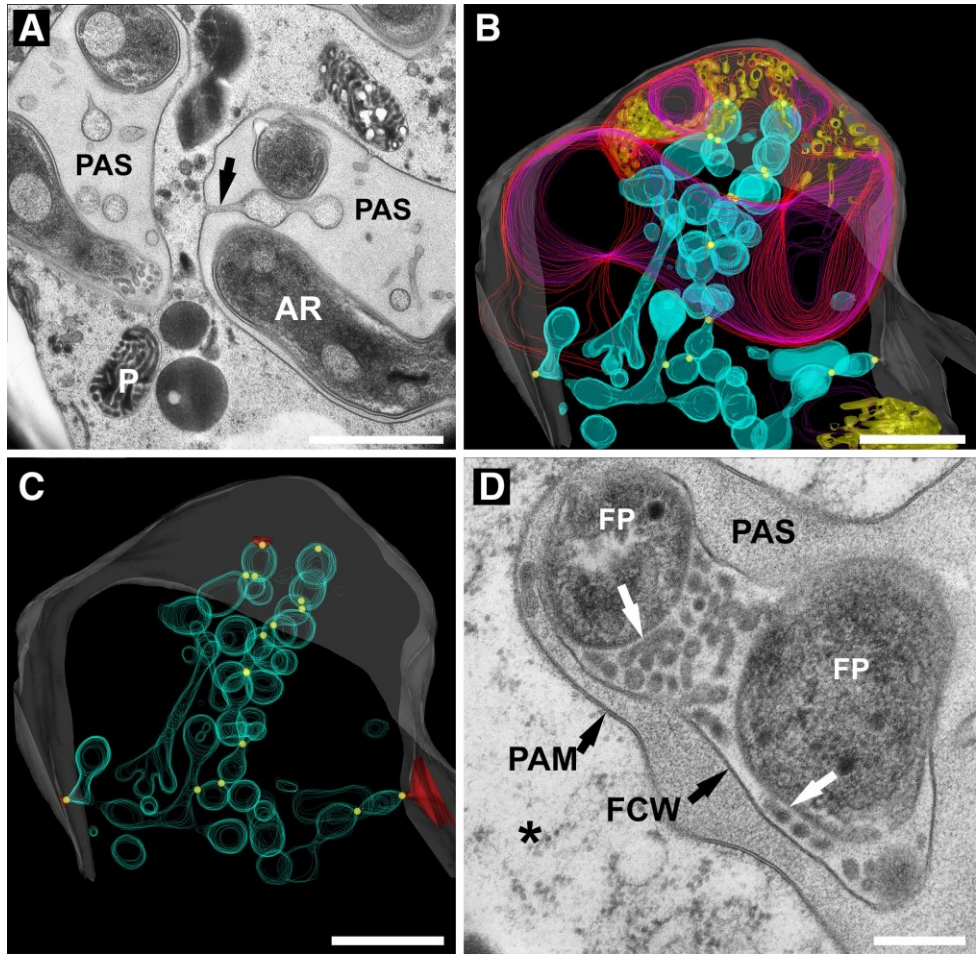


Fig. 4. Electron microscopy tomography of high-pressure frozen roots of *Medicago truncatula* colonized with *Rhizophagus irregularis*. **A,** A thin section of two groups of arbuscules (AR) surrounded by a region of enlarged periarbuscular space (PAS). Individual components did not appear interconnected when examined as thin sections. Note the intramatrix compartment (IMC) component docked at the periarbuscule membrane (arrow); P = plastid. Scale = 1 μm. **B,** Full model of a tomogram containing arbuscules. Supplementary Video S2 scrolls through stack of 528 slices used for the tomogram model and Supplementary Video S3 shows a rotation of modeled three-dimensional (3D) volume. The plant-derived membrane system within the interfacial IMC was visualized in cyan, fungal arbuscule tubules in yellow, the periarbuscule membrane in gray, the fungal protoplast in magenta, and the fungal cell wall in red. Scale = 500 nm. **C,** Same tomogram as that shown in B, emphasizing the distribution of narrow membrane pores (yellow spheres) throughout the IMC (cyan). In red are three regions of the periarbuscule membrane (PAM) from which the IMC originated and remains docked via pores. Supplementary Video S4 aids in understanding the 3D distribution of the pores. Modified from Ivanov et al. (2019). Scale = 500 nm. **D,** A thin section of fungal arbuscules with associated extracellular fungal tubules (white arrows) (*unpublished*). FP = fungal protoplast, FCW = fungal cell wall, PAS = interfacial matrix, asterisk = plant cytoplasm. Scale = 250 nm. Images and movies used with permission (Ivanov et al. 2019).

process that does not preserve all cellular components, and solvent dehydration extracts components and also causes shrinkage or swelling artifacts. Thin sections of this material showed ultrastructure that manifested these artifacts and the vesicles seen in the PAS were less prominent and easily ignored. However, cellular preservation was significantly improved by ultra-rapid freezing (Ivanov et al. 2019; Roth et al. 2019), all components of the system are fixed within a few milliseconds, and freezesubstitution removes tissue water in a frozen specimen, reducing shrinkage and swelling artifacts. Consequently, the matrix material of the PAS was not extracted and has a uniform distribution, giving membranes, including those of fungal tubules and the IMC, smooth profiles. In addition, resolving ultrastructure in 3D via ET of thick sections was shown here to be very helpful for understanding the function of these two membrane systems. Resin-embedded ET, until recently, was the most prevalent 3D approach for high-resolution studies of subcellular structures at the electron microscopy level. However, in 2017, the Nobel Prize in chemistry was awarded to a group of scientists who devel-

oped a group of cryo-electron microscopy techniques enabling the visualization of high-resolution structures (subnanometer) of frozen-hydrated biomolecules (Cressey and Callaway 2017; Henderson 2018). A rapidly growing variant, "cryoET" (Dillard et al. 2018; Doerr 2017), has now supplanted more traditional resin-based approaches and cryoET has now evolved to include in situ visualization of unstained biomolecule structures in frozen cells and tissues. A few important criteria must be met for successful in situ cellular cryoET. First, the sample must be vitrified (frozen without ice crystal damage) to eliminate the possibility that ice crystals distort the native cell structure.

Second, the sample must be sufficiently thin (about 200 nm) to create a tomogram tilt series, which is typically achieved by the creation of thin lamella via focused ion beam (FIB) milling. While plunge-freezing specimens on special TEM grids is sufficient for many unicellular organisms, such as for chloroplast structures in algae (Engel et al. 2015; Li et al. 2021), multiorganism and bulk tissues (Harapin et al. 2015; Mahamid et al. 2015) more analogous to most plant microbe-interactions will necessitate high-pressure freezing. A number of multiscale cryoET workflows now include the possibility to contextually image the unstained frozen cells and tissues via cryo-fluorescence, FIB-SEM 3D cryo serial block-face imaging, lamella creation, and then, finally, cryoET tomograms (Mahamid et al. 2015; Schaffer et al. 2019; Wu et al. 2020).

While ET is the highest-resolution approach to derive 3D structural information from cellular organelles, volumes created from a few 100-nm thick lamella can be limiting for understanding larger cellular features, entire cells, or tissues. This can be addressed with frozen samples, by alternating FIB surface milling and low voltage SEM imaging to create 3D datasets. Remarkable contrast can be achieved in the SEM of the unstained sample surface, which appears to be attributed to slight charge differences between the cell proteins, membranes, and vitrified ice (Schertel et al. 2013; Vidavsky et al. 2016). More recently, plasma FIB milling of cryo samples, using a user-selectable range of gasses (e.g., xenon, nitrogen, oxygen, argon) has shown great promise to further improve volume imaging and cryoET workflows (Dumoux et al. 2022) without fixation or metal staining, as demonstrated in chlamydomonas chloroplast (Fig. 5; Supplementary Video S5).

Alternatively, when specialized cryo-workflows are not available, a group of 3D resin-based methods can be used that enable acquisition of much larger volumes (hundreds of cubic micrometers) at nanoscale resolution with resin embedded samples, collectively termed volume electron microscopy (vEM) (Peddie and Collinson 2014) and touted by *Nature* as one of "seven technologies to watch in 2023" (Eisenstein 2023). While published re-

ports specific to plant-microbe interactions are lacking, thus far, the potential for vEM to serve as a workhorse for creating full 3D volumes of plant-microbe interaction sites cannot be overstated. Using classical conventional fixation and cryo-preservation followed by resin embedment, users can apply array tomography, which collects serial sections of target structures onto a rigid substrate (e.g., TEM grid, silicon wafer, coverslip) and images them using light microscopy with one or both TEM and SEM (Collman et al. 2015a; Delpiano et al. 2018; Mendenhall et al. 2017; Smith 2018). Alternatively, an intact resin block can be mounted and back-scatter SEM images can be acquired of the resin block face after repeatedly removing thin layers via an insitu microtome (serial block-face SEM) or surface ablation FIB-SEM (Bélanger et al. 2022; Czymmek et al. 2020; Harwood et al. 2019; Kittelmann et al. 2016; Oi et al. 2017). With volume SEM, detailed 3D spatial information is possible down to a few nanometers, although practically, imaging volumes are typically restricted to a maximum of a few hundred micrometers, due to the required acquisition times (up to days) and post-processing requirements. Notably, serial block-face vEM sample preparation often requires more prolonged and specialized fixation, staining, and embedding protocols, to ensure adequate signal-to-noise and beam-stable samples; however, these protocols are well-established and available to the community.

## Future Perspectives and Challenges

As described herein, select and sophisticated imaging tools and corresponding molecular and sample preparation methodologies were highlighted that have been demonstrated or have the potential to provide immediate and practical application to an array of plant-microbe studies. Collectively, they offer opportunities to generate one or more exquisite high-speed, high-resolution, multiscale, and multidimensional perspectives of symbiotic and disease states in plants. A decision point on which platform or platforms would be most appropriate to answer a specific biological question is highly dependent on the ultimate research objectives; however, a quick guide of major capabilities, limitations, length scales, and general applications are compared and contrasted in Table 1 and Figure 6 for your convenience.

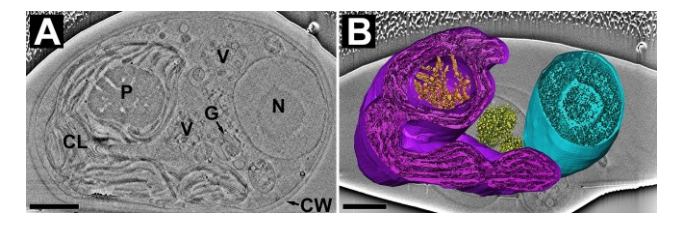


Fig. 5. Three-dimensional (3D) volume electron microscopy chlamydomonas dataset acquired on a Thermo Scientific Helios 5 Hydra plasmafocused ion beam scanning electron microscope. A, Single 5-nm resolution (x-y-z) secondary electron cryo block-face image of unstained chlamydomonas showed a complement of well-differentiated cell structures. N = nucleus, CL = chloroplast, P = pyrenoid, CW = cell wall, V = vacuoles, and G = Golgi. **B**, A 3D rendering of selected chlamydomonas organelles from A showed the chloroplast and its thylakoid membranes (purple), pyrenoid tubules (orange), Golgi (yellow), and nucleus (cyan). Scale bars =  $1 \mu M$ . We thank J. Plitzko (Max Planck Institute of Biochemistry) and A. Kotecha (Thermo Fisher Scientific) and team for permission to use underlying data deposited on the electron microscopy public image archive (EMPIAR-11275). This data was processed using Thermo Fisher Scientific Amira and, specifically, the deep learning modules for segmentation. Amira software was also used to generate 3D visualizations, post-process the data, and characterize the sample. We thank R. Chalmers, M. McClendon, and Thermo Fisher's Visualization and Data Sciences group for their support and work on the

Additional approaches worth watching that do not neatly fit in the approaches described above, such as correlative microscopy, essentially imaging the same sample with multiple imaging modalities, continue to evolve and also will provide important contributions to the field. One form, commonly known as CLEM (correlative light and electron microscopy), has seen increasing tools and applications in plants, microbes, and their interactions (Caplan et al. 2011; Marion et al. 2017; Modla et al. 2015; Weiner et al. 2022). Ultimately, correlative microscopy can combine the benefits of two different approaches, such as visualizing the chemical specificity of florescent probes, overlaid onto the ul-

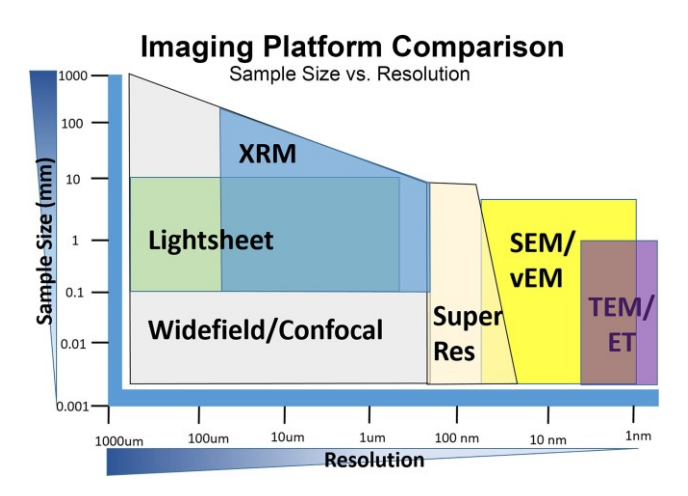


Fig. 6. Imaging platform comparison (sample size versus resolution). This figure shows the relative sample sizes possible and common imaging platform resolution ranges to help guide appropriate selection for specific biological questions including X-ray microscopy (XRM), widefield and confocal microscopy, lightset microscopy, super-resolution microscopy (Super Res), scanning electron microscopy (SEM) and volume electron microscopy (vEM), and transmission electron microscopy (TEM) and electron tomography (ET). Adopted and modified from Zeiss Microscopy 3D microscopy applications.

trastructural information provided from electron microscopy. In the extreme implementation, super-resolution images of fluorescent protein fusions can be acquired at cryogenic temperatures, and the sample can subsequently be processed for volume FIB-SEM and merged into pixel-precise merged 3D volumes (Hoffman et al. 2020). More broadly speaking, there are numerous other suitable ways to mix and match between localization microscopy, electron microscopy, and XRM protocols for 2D and 3D integration of multimodal and multiscale datasets (Caplan et al. 2011; Duncan et al. 2022; Mitchell et al. 2021).

Additionally, spatial-omics techniques (Chen et al. 2020, Giacomello and Lundeberg 2018; Salmén et al. 2018) are rapidly advancing and transforming the way we understand complex organisms and their interactions with the environment and are increasingly explored in plants. One form, "multiplex" microscopy, has been increasingly applied for biomedical applications in complex tissue systems to understand human disease (i.e., cancer, clinical diagnostics, connectomics) (Collman et al. 2015b; Tan et al. 2020; Xia et al. 2019). Multiplex microscopy simultaneously or sequentially visualizes an extended array of biomolecular probes on single sections or cell monolayers, thus providing high-dimensional physical mapping of numerous cellular phenotypes and components over heterogeneous tissues, and complements other high-resolution omics such as single-cell sequencing. Despite the fact that plants pose unique challenges (i.e. cell walls, large air or vacuolar spaces), there has been some limited adoption (i.e., small RNA and messenger RNA localization in paraffin sections [Huang et al. 2019, 2020]). However, we expect that the utility of this approach will experience increased value in plant-microbe interactions as the technique evolves, especially when combining precise localization of any array of chemically specific fluorescent probes with ultrastructural fea-

While opportunity abounds, it must be noted that there remain significant barriers and caveats for routine use to provide high-quality outcomes and ultimately broad adoption of advanced microscopy approaches. First, limited availability and affordability, especially for more specialized technologies such as cryoET,

Table 1. Imaging platform comparison of key capabilities and general applications

Platform	Resolution (lateral)	Advantages	Disadvantages	Applications
Widefield	250 nm	Lowest cost, rapid screening, work-horse approach	Bulk/thick/deep plant tissues more difficult	Histology, in situ hybridization, classical stains/protocols. Sectioned tissues
Confocal	120 nm	3D optical sectioning of fixed and live specimen, thick plant tissues	Point scanning systems can be slow	Fluorescent protein tagged probes of microbes, pathogens, and interactions
Lightsheet	500 nm	3D optical section of live and cleared tissues; fast acquisition	Resolution reduced compared with point scanning	Development and morphology studies
Super-resolution	20 nm	Single molecule sensitivity; highest resolution photon-based imaging	Typically requires postprocessing of multiple images (can be slow)	Suborganelle targets over large areas
X-ray tomography	100 nm to mm	3D imaging of intact, delicate, or complicated samples over multiple scales, or both	Often requires exogenous contrast agents; probe localization and suborganelle resolution not yet demonstrated in plant samples	Phenotyping, development and morphology; aid to volume electron microscopy in correlative workflows
Transmission electron microscopy	0.2 nm	Highest resolution 2D imaging; most proteins and membranes visible	Fixed/dead cells; small sample size	Cell/organelle ultrastructure (e.g., mutants, plant-microbe interactions)
Electron tomography	About 1 nm	Highest resolution 3D imaging; cryo and conventional preps possible	Complex sample preparation; restricted sample size; vitrification required for cryo-prep	Structural biology of cell organelles, supra-molecular assemblies, multiprotein structures, and viruses
Scanning electron microscopy	0.5 to 5 nm	High-resolution surface imaging and atomic contrast	Dead/fixed samples; surface only	Plant-microbe interactions and high-resolution plant/microbe surface imaging
Volume electron microscopy	About 3 nm	Nanoscale resolution; isotropic voxels possible	Complex sample preparation	3D ultrastructural imaging and quantification of whole organelles, cells, and tissues

super-resolution, vEM, and beamline synchrotron XRT. Many of these platforms are not universally accessible at smaller, midsize, or even some large institutions. From a practical standpoint, to purchase, maintain, and operate these high-end systems require a critical mass of investigators with clear scientific need in order to justify ownership. Furthermore, when available, technical operators very often lack specific expertise in preparing, handling, or interpreting results from plants or microbe samples.

From a sample handling and imaging perspective, specialized techniques using cryo-preservation have limits in applicable tissue size (typically less than a few hundred micrometers) and are prone to artifacts related to the freezing process itself, such as sample-dependent ice crystal formation, devitrification, pressurization, mechanical damage, space-filler effects, to name just a few. Likewise, conventional chemical fixation, depend-

ing on the nature of the biological question and the imaging platform applied, may be the most appropriate approach, with the caveat of known artifacts due to aldehyde fixation, osmotic and buffer effects, and very slow and limited penetration of fixatives and chemical reagents into thick plant and microbial tissues or systems. For live-cell work, steps should be taken to ensure the tissues are consistently prepared, not overly manipulated or stressed (including light-induced phototoxicity and environmental changes), and best reflect the biology being measured. For example, does overexpression of fusion proteins alter biological function? Does extraction of a root from the soil or excision of a leaf from the intact plant alter the context of its local environment? Informed consideration and appropriate understanding of the nuances of plant and microbial sample preparation, their fundamental cell structure and biology, and potential imaging and molecular artifacts must be carefully considered when interpreting results. Addressing these realities may also help resolve the controversial research area of plant-based apoplastic extracellular vesicles (EVs) (Pinedo et al. 2021) and whether they are nonartifactual and biologically relevant structures in walled plants and fungi. The uncertainty of the origin of EVs is compounded by the lack of compelling high-quality and direct in planta evidence (3D likely would be required) that shows definitive cell wall transit to the apoplast. Furthermore, a reasonable mechanism must be defined that would permit numerous approximately 150-nm EVs (Rutter and Innes 2017) to transit and be released into plant extracellular airspaces despite the fact that the effective plant cell-wall pore size typically ranges between about 3.5 to 8.5 nm (Carpita et al. 1979; Read and Bacic 1996; Proseus and Boyer 2005). Regardless of approach, such molecular or microscopy studies must be viewed with caution, as we apply our very best efforts to unequivocally ensure we are not measuring the artifactual release of cytoplasmic vesicles, as plants and fungal cells are prone to micro breaks or rupture during sample processing from osmotic effects or infiltration or extraction studies. Under the right conditions, it seems advanced microscopy could help address these gaps.

Ultimately, for the reasons mentioned above, this may necessitate more opportunities for training scientists to understand the potential and appropriate applications, limitations, and pitfalls of these advanced microscopy tools for focused plant-microbe studies. This would include fundamental and advanced platform and workflow training (e.g., sample preparation, data acquisition, image processing, statistically relevant quantification and interpretation), and we highly encourage cross-disciplinary collaborations in which experts in respective areas support the successful, well designed, controlled, and robust experimental outcomes.

Finally, there is often no substitute for the incorporation of routine microscopy to screen samples, augment molecular and genomic studies, and provide important and critical insights into the mechanisms of plant-microbe interactions. When a deeper understanding is warranted, a multitude of powerful techniques and imaging technologies are already at hand and many described herein can be applied. Some are more accessible (e.g., confocal microscopy and fluorescent protein expression), while others are much less common, require technical resources, or have complex workflows (Table 1), including, but not limited to, XRM, cryoET, AO. We anticipate a number of these more specialized approaches will become more mainstream, cost effective, and improve their usability in the very near future. Nevertheless, and regardless of approach to solve pressing biological questions, the benefits of these tools remain largely underutilized in the field, yet their potential to further substantially benefit and propel our fundamental knowledge of plant-microbe interactions forward is essentially limitless.

## Acknowledgments

We thank J. Plitzko (Max Planck Institute of Biochemistry) and A. Kotecha (Thermo Fisher Scientific) for the cryo 3D chlamydomonas dataset (EMPIAR-11275) and M. McClendon, R. Chalmers and Thermo Fisher Scientific Visualization and Data Sciences group for their support using Amira and deep learning tools for segmentation of that data.

### **Literature Cited**

- Bayguinov, P. O., Fisher, M. R., and Fitzpatrick, J. A. J. 2020. Assaying three-dimensional cellular architecture using X-ray tomographic and correlated imaging approaches. J. Biol. Chem. 295:15782-15793.
- Bélanger, S., Berensmann, H., Baena, V., Duncan, K., Meyers, B. C., Narayan, K., and Czymmek, K. J. 2022. A versatile enhanced freezesubstitution protocol for volume electron microscopy. Front. Cell Dev. Biol. 10:933376.
- Benhamou, N., and Bélanger, R. 2017. Immunoelectron microscopy. Pages 15-29 in: Molecular Methods in Plant Pathology. CRC Press, Boca Raton, FL, U.S.A.
- Berg, R. H., and Beachy, R. N. 2008. Fluorescent Protein Applications in Plants. Methods Cell Biol. 85:153-177.
- Betzig, E., Patterson, G. H., Sougrat, R., Lindwasser, O. W., Olenych, S., Bonifacino, J. S., Davidson, M. W., Lippincott-Schwartz, J., and Hess, H. F. 2006. Imaging intracellular fluorescent proteins at nanometer resolution. Science 313:1642-1645.
- Bloemberg, G. V., Wijfjes, A. H. M., Lamers, G. E. M., Stuurman, N., and Lugtenberg, B. J. J. 2000. Simultaneous imaging of *Pseudomonas fluo*rescens WCS365 populations expressing three different autofluorescent proteins in the rhizosphere: New perspectives for studying microbial communities. Mol. Plant-Microbe Interact. 13:1170-1176.
- Bonfante-Fasolo, P. 1987. Vesicular-arbuscular mycorrhizae: fungus-plant interactions at the cellular level. Symbiosis 3:249-268.
- Bortolami, G., Gambetta, G. A., Delzon, S., Lamarque, L. J., Pouzoulet, J.,
  Badel, E., Burlett, R., Charrier, G., Cochard, H., Dayer, S., Jansen, S.,
  King, A., Lecomte, P., Lens, F., Torres-Ruiz, J. M., and Delmas, C. E. L.
  2019. Exploring the hydraulic failure hypothesis of esca leaf symptom formation. Plant Physiol. 181:1163-1174.
- Bougourd, S., Marrison, J., and Haseloff, J. 2000. An aniline blue staining procedure for confocal microscopy and 3D imaging of normal and perturbed cellular phenotypes in mature *Arabidopsis* embryos. Plant J. 24:543-550.
- Bourett, T. M., and Howard, R. J. 1990. In vitro development of penetration structures in the rice blast fungus *Magnaporthe grisea*. Can. J. Bot. 68:329-342.
- Bourett, T. M., Sweigard, J. A., Czymmek, K. J., Carroll, A., and Howard, R. J. 2002. Reef coral fluorescent proteins for visualizing fungal pathogens. Fungal Genet. Biol. 37:211-220.
- Brar, G. S., Karunakaran, C., Bond, T., Stobbs, J., Liu, N. a, Hucl, P. J., and Kutcher, H. R. 2019. Showcasing the application of synchrotron-based X-ray computed tomography in host-pathogen interactions: The role of wheat rachilla and rachis nodes in type-II resistance to *Fusarium graminearum*. Plant Cell Environ. 42:509-526.
- Caplan, J., Niethammer, M., Taylor, R. M., and Czymmek, K. J. 2011. The power of correlative microscopy: Multi-modal, multi-scale, multi-dimensional. Curr Opin Struc. Biol. 21:686-693.
- Cardinale, M., and Berg, G. 2015. Visualization of Plant-Microbe Interactions. Pages 299-306 in: Principles of Plant-Microbe Interactions. Springer International Publishing, Cham, Switzerland.

- Carpita, N., Sabularse, D., Montezinos, D., and Delmer, D. P. 1979. Determination of the pore size of cell walls of living plant cells. Science 205:1144-1147.
- Cattoni, D., Fiche, J., and Nöllmann, M. 2012. Single-molecule super-resolution imaging in bacteria. Curr. Opin. Microbiol. 15: 758-763.
- Chalfie, M., Tu, Y., Euskirchen, G., Ward, W. W., and Prasher, D. C. 1994. Green fluorescent protein as a marker for gene expression. Science 263:802-805.
- Chang, J.-B., Chen, F., Yoon, Y.-G., Jung, E. E., Babcock, H., Kang, J. S., Asano, S., Suk, H.-J., Pak, N., Tillberg, P. W., Wassie, A. T., Cai, D., and Boyden, E. S. 2017. Iterative expansion microscopy. Nat. Methods 14:593-599.
- Chen, F., Tillberg, P. W., and Boyden, E. S. 2015. Expansion microscopy. Science 347:543-548.
- Chen, J., Gutjahr, C., Bleckmann, A., and Dresselhaus, T. 2015. Calcium signaling during reproduction and biotrophic fungal interactions in plants. Mol. Plant 8:595-611.
- Chen, W.-T., Lu, A., Craessaerts, K., Pavie, B., Sala Frigerio, C., Corthout, N., Qian, X., Laláková, J., Kühnemund, M., Voytyuk, I., Wolfs, L., Mancuso, R., Salta, E., Balusu, S., Snellinx, A. n, Munck, S., Jurek, A., Fernandez Navarro, J., Saido, T. C., Huitinga, I., Lundeberg, J., Fiers, M., and De Strooper, B. 2020. Spatial transcriptomics and in situ sequencing to study Alzheimer's disease. Cell 182:976-991.e19.
- Ckurshumova, W., Caragea, A. E., Goldstein, R. S., and Berleth, T. 2011 Glow in the dark: Fluorescent proteins as cell and tissue-specific markers in plants. Mol. Plant 4:794-804.
- Collman, F., Buchanan, J., Phend, K. D., Micheva, K. D., Weinberg, R. J., and Smith, S. J. 2015a. Mapping synapses by conjugate light-electron array tomography. J. Neurosci. 35:5792-5807.
- Collman, F., Buchanan, J., Phend, K. D., Micheva, K. D., Weinberg, R. J., and Smith, S. J. 2015b. Mapping synapses by conjugate light-electron array tomography. J. Neurosci. 35:5792-5807.
- Cox, G., and Sanders, F. 1974. Ultrastructure of the host-fungus interface in a vesicular-arbuscular mycorrhiza. New Phytol. 73:901-912.
- Cressey, D., and Callaway, E. 2017. Cryo-electron microscopy wins chemistry Nobel. Nature 550:167-167.
- Cui, Y., Zhao, Y., Lu, Y., Su, X., Chen, Y., Shen, Y., Lin, J., and Li, X. 2021. In vivo single-particle tracking of the aquaporin AtPIP2;1 in stomata reveals cell type-specific dynamics. Plant Physiol. 185:1666-1681.
- Czymmek, K., Sawant, A., Goodman, K., Pennington, J., Pedersen, P., Hoon, M., and Otegui, M. S. 2020. Imaging plant cells by high-pressure freezing and serial block-face scanning electron microscopy. Pages 69-81 in: Plant Endosomes. Methods in Molecular Biology. Vol. 2177. M. S. Ortegui, ed. Humana, New York.
- Czymmek, K. J., Bourett, T. M., Sweigard, J. A., Carroll, A., and Howard, R. J. 2002. Utility of cytoplasmic fluorescent proteins for live-cell imaging of *Magnaporthe grisea* in planta. Mycologia 94:280-289.
- Czymmek, K. J., Fogg, M., Powell, D. H., Sweigard, J., Park, S.-Y., and Kang, S. 2007. In vivo time-lapse documentation using confocal and multi-photon microscopy reveals the mechanisms of invasion into the *Arabidopsis* root vascular system by *Fusarium oxysporum*. Fungal Genet. Biol. 44:1011-1023.
- Czymmek, K. J., Whallon, J. H., and Klomparens, K. L. 1994. Confocal microscopy in mycological research. Exp. Mycol. 18:275-293.
- Delpiano, J., Pizarro, L., Peddie, C. J., Jones, M. L., Griffin, L. D., and Collinson, L. M. 2018. Automated detection of fluorescent cells in inresin fluorescence sections for integrated light and electron microscopy. J. Microsc. 271:109-119.
- Dexheimer, J., Marx, C., Gianinazzi-Pearson, V., and Gianinazzi, S. 1985. Ultracytological studies of plasmalemma formations produced by host and fungus in vesicular-arbuscular mycorrhizae. Cytologia (Tokyo) 50:461-471.
- Dillard, R. S., Hampton, C. M., Strauss, J. D., Ke, Z., Altomara, D., Guerrero-Ferreira, R. C., Kiss, G., and Wright, E. R. 2018. Biological applications at the cutting edge of cryo-electron microscopy. Microsc. Microanal. 24:406-419.
- Doerr, A. 2017. Cryo-electron tomography. Nat. Methods 14:34-34.
  Dumoux, M., Glen, T., Ho, E. M. L., Perdigão, L. M. A., Klumpe, S., Yee, N. B. Y., Farmer, D., Smith, J. L. R., Yiu, P., Lai, A., Bowles, W., Kelley, R., Plitzko, J. M., Wu, L., Basham, M., Clare, D. K., Siebert, C. A., Darrow, M. C., Naismith, J. H., and Grange, M. 2022 Cryo-plasma FIB /SEM volume imaging of biological specimens structural biology. bioRxiv. doi:10.1101/2022.09.21.508877.
- Duncan, K. E., Czymmek, K. J., Jiang, N. i, Thies, A. C., and Topp, C. N. 2022. X-ray microscopy enables multiscale high-resolution 3D imaging of plant cells, tissues, and organs. Plant Physiol. 188: 831-845.

- Eder, M., and Lutz-Meindel, U. 2008. Pectin-like carbohydrates in the green alga *Micrasterias* characterized by cytochemical analysis and energy filtering TEM. J. Microsc. 231:201-214.
- Eisenstein, M. 2023. Seven technologies to watch in 2023. Nature 613: 794-797.
- Engel, B. D., Schaffer, M., Kuhn Cuellar, L., Villa, E., Plitzko, J. M., and Baumeister, W. 2015. Native architecture of the Chlamydomonas chloroplast revealed by in situ cryo-electron tomography. eLife 4: e04889.
- Gahlmann, A., and Moerner, W. E. 2014. Exploring bacterial cell biology with single-molecule tracking and super-resolution imaging. Nat. Rev. Microbiol. 12:9-22.
- Giacomello, S., and Lundeberg, J. 2018. Preparation of plant tissue to enable spatial transcriptomics profiling using barcoded microarrays. Nat. Protoc. 13:2425-2446.
- Gianinazzi-Pearson, V., Morandi, D., Dexheimer, J., and Gianinazzi, S. 1981. Ultrastructural and ultracytochemical features of a *Glomus tenuis* mycorrhiza. New Phytol. 88:633-639.
- Gilkey, J. C., and Staehelin, L. A. 1986. Advances in ultrarapid freezing for the preservation of cellular ultrastructure. J. Electron Microsc. Tech. 3:177-210.
- Götz, R., Panzer, S., Trinks, N., Eilts, J., Wagener, J., Turrà, D., Di Pietro, A., Sauer, M., and Terpitz, U. 2020. Expansion microscopy for cell biology analysis in fungi. Front. Microbiol. 11:00574.
- Gustafsson, M. G. L. 2000 Surpassing the lateral resolution limit by a factor of two using structured illumination microscopy. J. Microsc. 198: 82-87.
- Hampson, K. M., Turcotte, R., Miller, D. T., Kurokawa, K., Males, J. R., Ji, N., and Booth, M. J. 2021. Adaptive optics for high-resolution imaging. Nat. Rev. Methods Primers 1:68.
- Harapin, J., Börmel, M., Sapra, K. T., Brunner, D., Kaech, A., and Medalia, O. 2015. Structural analysis of multicellular organisms with cryo-electron tomography. Nat. Methods 12:634-636.
- Hardham, A. R. 2012. Confocal microscopy in plant-pathogen interactions. Methods Mol. Biol. 835:295-309.
- Harwood, R., Goodman, E., Gudmundsdottir, M., Huynh, M., Musulin, Q., Song, M., and Barbour, M. M. 2019. Cell and chloroplast anatomical features are poorly estimated from 2D cross-sections. New Phytol. 225: 2567-2578.
- Henderson, R. 2018. From electron crystallography to single particle cryoEM (Nobel lecture). Angewandte Chemie 57:10804-10825.
- Henty-Ridilla, J. L., Shimono, M., Li, J., Chang, J. H., Day, B., and Staiger, C. J. 2013. The plant actin cytoskeleton responds to signals from microbeassociated molecular patterns. PLoS Path. 9:e1003290.
- Hepler, P. K., and Gunning, B. E. S. 1998. Confocal fluorescence microscopy of plant cells. Protoplasma 201:121-157.
- Hickey, P. C., Swift, S. R., Roca, M. G., and Read, N. D. 2004. Live-cell imaging of filamentous fungi using vital fluorescent dyes and confocal microscopy. Methods Microbiol. 34:63-87.
- Hoffman, D. P., Shtengel, G., Xu, C. S., Campbell, K. R., Freeman, M., Wang, L., Milkie, D. E., Pasolli, H. A., Iyer, N., Bogovic, J. A., Stabley, D. R., Shirinifard, A., Pang, S., Peale, D., Schaefer, K., Pomp, W., Chang, C.-L., Lippincott-Schwartz, J., Kirchhausen, T., Solecki, D. J., Betzig, E., and Hess, H. F. 2020. Correlative three-dimensional super-resolution and block-face electron microscopy of whole vitreously frozen cells. Science 367:6475.
- Hohmann-Marriott, M. F., Uchida, M., Van De Meene, A. M. L., Garret, M., Hjelm, B. E., Kokoori, S., and Roberson, R. W. 2006. Application of electron tomography to fungal ultrastructure studies. New Phytol. 172: 208-220.
- Hou, L. (H.)., Gao, W., der Bom, F., Weng, Z. (H.), Doolette, C. L., Maksimenko, A., Hausermann, D., Zheng, Y., Tang, C., Lombi, E., and Kopittke, P. M. 2022. Use of X-ray tomography for examining root architecture in soils. Geoderma 405;115405.
- Howard, R. J. 1981. Ultrastructural analysis of hyphal tip cell growth in fungi: Spitzenkorper, cytoskeleton and endomembranes after freezesubstitution. J. Cell Sci. 48:89-103.
- Huang, B., Babcock, H., and Zhuang, X. 2010. Breaking the diffraction barrier: Super-resolution imaging of cells. Cell 143:1047-1058.
- Huang, K., Baldrich, P., Meyers, B. C., and Caplan, J. L. 2019. sRNA-FISH: Versatile fluorescent in situ detection of small RNAs in plants. Plant J. 98:359-369.
- Huang, K., Demirci, F., Batish, M., Treible, W., Meyers, B. C., and Caplan, J. L. 2020. Quantitative, super-resolution localization of small RNAs with sRNA-PAINT. Nucleic Acids Res. 48:e96.
- Ingel, B., Caldwell, D., Duong, F., Parkinson, D. Y., McCulloh, K. A., Iyer-Pascuzzi, A. S., McElrone, A. J., and Lowe-Power, T. M. 2022. Revisiting the source of wilt symptoms: X-ray microcomputed tomography provides

- direct evidence that *Ralstonia* biomass clogs xylem vessels. PhytoFrontiers 2:41-51.
- Ivanov, S., Austin, J., Berg, R. H., and Harrison, M. J. 2019. Extensive membrane systems at the host–arbuscular mycorrhizal fungus interface. Nat. Plants 5:194-203.
- Jabusch, L. K., Kim, P. W., Chiniquy, D., Zhao, Z., Wang, B., Bowen, B., Kang, A. J., Yoshikuni, Y., Deutschbauer, A. M., Singh, A. K., and Northen, T. R. 2021. Microfabrication of a chamber for high-resolution, in situ imaging of the whole root for plant-microbe interactions. Int. J. Mol. Sci. 22:7880.
- Jacobsen, C. 2019. X-ray Microscopy (Advances in Microscopy and Microanalysis). Cambridge University Press, Cambridge. doi:10.1017/9781139924542.
- Jeffree, C. E., and Read, N. D. R. 1991. Ambient- and low-temperature scanning electron microscopy. Electron Microscopy of Plant Cells. C. Hall and J. L. Hawes, eds. Academic Press, London.
- Kankanala, P., Czymmek, K., and Valent, B. 2007. Roles for rice membrane dynamics and plasmodesmata during biotrophic invasion by the blast fungus. Plant Cell 19:706-724.
- Kao, P., and Nodine, M. D. 2021. Application of expansion microscopy on developing Arabidopsis seeds. Methods Cell Biol. 161:181-195.
- Kausche, G. A., Pfankuch, E., and Ruska, H. 1939. Die Sichtbarmachung von pflanzlichem virus im Übermikroskop. Naturwissenschaften 27: 292-299.
- Keller, P. J., and Dodt, H.-U. 2012. Light sheet microscopy of living or cleared specimens. Curr. Opin. Neurobiol. 22:138-143.
- Keyes, S., Veelen, A., McKay Fletcher, D., Scotson, C., Koebernick, N., Petroselli, C., Williams, K., Ruiz, S., Cooper, L., Mayon, R., Duncan, S., Dumont, M., Jakobsen, I., Oldroyd, G., Tkacz, A., Poole, P., Mosselmans, F., Borca, C., Huthwelker, T., Jones, D. L., and Roose, T. 2022. Multimodal correlative imaging and modelling of phosphorus uptake from soil by hyphae of mycorrhizal fungi. New Phytol. 234:688-703.
- Keyes, S. D., Gostling, N. J., Cheung, J. H., Roose, T., Sinclair, I., and Marchant, A. 2017. The application of contrast media for in vivo feature enhancement in X-Ray computed tomography of soil-grown plant roots. Microsc. Microanal. 23:538-552.
- Khang, C. H., Berruyer, R., Giraldo, M. C., Kankanala, P., Park, S.-Y., Czymmek, K., Kang, S., and Valent, B. 2010. Translocation of *Magnaporthe oryzae* effectors into rice cells and their subsequent cell-to-cell movement. Plant Cell 22:1388-1403.
- Kim, H.-S., Park, S.-Y., Kang, S., and Czymmek, K. J. 2022. Time-lapse imaging of root pathogenesis and fungal proliferation without physically disrupting roots. Pages 153-170 in: Fusarium Wilt. Methods in Molecular Biology, Vol. 2391. Humana, New York.
- Kittelmann, M., Hawes, C., and Hughes, L. 2016. Serial block face scanning electron microscopy and the reconstruction of plant cell membrane systems. J. Microsc. 263:200-211.
- Komarov, S., and Tai, Y.-C. 2022. Positron emission tomography (PET) for molecular plant imaging. Pages 97-118 in: High-Throughput Plant Phenotyping. Methods in Molecular Biology, Vol. 2539. Humana, New York.
- Komis, G., Šamajová, O., Ovec ka, M., and Šamaj, J. 2015. Super-resolution microscopy in plant cell imaging. Trends Plant Sci. 20:834-843.
- Kumar, A. S., Lakshmanan, V., Caplan, J. L., Powell, D., Czymmek, K. J., Levia, D. F., and Bais, H. P. 2012. Rhizobacteria *Bacillus subtilis* restricts foliar pathogen entry through stomata. Plant J. 72:694-706.
- Kurihara, D., Mizuta, Y., Sato, Y., and Higashiyama, T. 2015. ClearSee: A rapid optical clearing reagent for whole-plant fluorescence imaging. Development 142:4168-4179.
- Lammel, D. R., Arlt, T., Manke, I., and Rillig, M. C. 2019. Testing contrast agents to improve micro computerized tomography (μCT) for spatial location of organic matter and biological material in soil. Front. Environ. Sci. 7:1-10.
- Leeuwenhoek, A. V. 1673. A specimen of some observations made by a microscope, contrived by M. Leewenhoeck in Holland, lately communicated by Dr. Regnerus de Graaf. Philos. T. R. Soc. Lond. 8:6037-6038.
- Li, M., Ma, J., Li, X., and Sui, S.-F. 2021. In situ cryo-ET structure of phycobilisome-photosystem II supercomplex from red alga. eLife 10:10.
- Li, Y.-B., Xu, R., Liu, C., Shen, N., Han, L.-B., and Tang, D. 2020. *Magna-porthe oryzae* fimbrin organizes actin networks in the hyphal tip during polar growth and pathogenesis. PLOS Pathog. 16:e1008437.
- Libault, M., Govindarajulu, M., Berg, R. H., Ong, Y. T., Puricelli, K., Taylor, C. G., Xu, D., and Stacey, G. 2011. A dual-targeted soybean protein is involved in *Bradyrhizobium japonicum* infection of soybean root hair and cortical cells. Mol. Plant-Microbe Interact. 24:1051-1060.
- Littlejohn, G. R., Gouveia, J. D., Edner, C., Smirnoff, N., and Love, J. 2010. Perfluorodecalin enhances in vivo confocal microscopy resolution of *Arabidopsis thaliana* mesophyll. New Phytol. 186:1018-1025.

- Littlejohn, G. R., Mansfield, J. C., Christmas, J. T., Witterick, E., Fricker, M. D., Grant, M. R., Smirnoff, N., Everson, R. M., Moger, J., and Love, J. 2014. An update: Improvements in imaging perfluorocarbon-mounted plant leaves with implications for studies of plant pathology, physiology, development and cell biology. Front. Plant Sci. 5:1-8.
- Liu, T.-L., Upadhyayula, S., Milkie, D. E., Singh, V., Wang, K., Swinburne, I. A., Mosaliganti, K. R., Collins, Z. M., Hiscock, T. W., Shea, J., Kohrman, A. Q., Medwig, T. N., Dambournet, D., Forster, R., Cunniff, B., Ruan, Y., Yashiro, H., Scholpp, S., Meyerowitz, E. M., Hockemeyer, D., Drubin, D. G., Martin, B. L., Matus, D. Q., Koyama, M., Megason, S. G., Kirchhausen, T., and Betzig, E. 2018. Observing the cell in its native state: Imaging subcellular dynamics in multicellular organisms. Science 360:aaq1392.
- Loconte, V., Singla, J., Li, A., Chen, J.-H., Ekman, A., McDermott, G., Sali, A., Le Gros, M., White, K. L., and Larabell, C. A. 2022. Soft X-ray tomography to map and quantify organelle interactions at the mesoscale. Structure 30:510-521.e3.
- Mahamid, J., Schampers, R., Persoon, H., Hyman, A. A., Baumeister, W., and Plitzko, J. M. 2015. A focused ion beam milling and lift-out approach for site-specific preparation of frozen-hydrated lamellas from multicellular organisms. J. Struc. Biol. 192:262-269.
- Marion, J., Le Bars, R., Satiat-Jeunemaitre, B., and Boulogne, C. 2017. Optimizing CLEM protocols for plants cells: GMA embedding and cryosections as alternatives for preservation of GFP fluorescence in *Arabidopsis* roots. J. Struc. Biol. 198:196-202.
- Martell, J. D., Deerinck, T. J., Lam, S. S., Ellisman, M. H., and Ting, A. Y. 2017. Electron microscopy using the genetically encoded APEX2 tag in cultured mammalian cells. Nat. Protoc. 12:1792-1816.
- Martino, E., Murat, C., Vallino, M., Bena, A., Perotto, S., and Spanu, P. 2007. Imaging mycorrhizal fungal transformants that express EGFP during ericoid endosymbiosis. Curr. Genet. 52:65-75.
- Marx, V. 2017. Microscopy: Hello, adaptive optics. Nat. Methods 14: 1133-1136.
- Mendenhall, J. M., Kuwajima, M., and Harris, K. M. 2017. Automated serial section large-field transmission-mode scanning electron microscopy (tSEM) for volume analysis of hippocampus ultrastructure. Microsc. Microanal. 23:562-563.
- Mendgen, K., and Lesemann, D.-E. 1991. Electron Microscopy of Plant Pathogens. Springer, Berlin.
- Mendgen, K., Welter, K., Scheffold, F., and Knauf-Beiter, G. 1991. High pressure freezing of rust infected plant leaves. Pages 31-42 in: Electron Microscopy of Plant Pathogens. K. Mendgen and D. E. Lesemann, eds. Springer, Berlin.
- Mendoza-Suárez, M. A., Geddes, B. A., Sánchez-Cañizares, C., Ramírez-González, R. H., Kirchhelle, C., Jorrin, B., and Poole, P. S. 2020. Optimizing *Rhizobium*-legume symbioses by simultaneous measurement of rhizobial competitiveness and N<sub>2</sub> fixation in nodules. Proc. Natl. Acad. Sci. U.S.A. 117:9822-9831.
- Mennella, V., and Liu, Z. 2022. Nanometer-scale molecular mapping by super-resolution fluorescence microscopy. Pages 305-326 in: Fluorescent Microscopy. Methods in Molecular Biology, Vol. 2440. Humana, New York.
- Metscher, B. D., and Müller, G. B. 2011. MicroCT for molecular imaging: Quantitative visualization of complete three-dimensional distributions of gene products in embryonic limbs. Dev. Dyn. 240:2301-2308.
- Mims, C. W., Rodriguez-Lother, C., and Richardson, E. A. 2002. Ultrastructure of the host-pathogen interface in daylily leaves infected by the rust fungus *Puccinia hemerocallidis*. Protoplasma 219:221-226.
- Mitchell, R. L., Davies, P., Kenrick, P., Volkenandt, T., Pleydell-Pearce, C., and Johnston, R. 2021. Correlative microscopy: A tool for understanding soil weathering in modern analogues of early terrestrial biospheres. Sci. Rep. 11:12736.
- Mizuta, Y. 2021. Advances in two-photon imaging in plants. Plant Cell Physiol. 62:1224-1230.
- Mizuta, Y., Kurihara, D., and Higashiyama, T. 2015, Two-photon imaging with longer wavelength excitation in intact *Arabidopsis* tissues. Protoplasma 252:1231-1240.
- Modla, S., Caplan, J. L., Czymmek, K. J., and Lee, J.-Y. 2015. Localization of fluorescently tagged protein to plasmodesmata by correlative light and electron microscopy. In: Plasmodesmata. Methods in Molecular Biology, Vol. 1217. M. Heinlein, ed. Humana Press, New York.
- Naim, F., Khambatta, K., Sanglard, L. M. V. P., Sauzier, G., Reinhardt, J., Paterson, D. J., Zerihun, A., Hackett, M. J., and Gibberd, M. R. 2021. Synchrotron X-ray fluorescence microscopy-enabled elemental mapping illuminates the "battle for nutrients" between plant and pathogen. J. Exp. Bot. 72:2757-2768.
- Ng, J., Browning, A., Lechner, L., Terada, M., Howard, G., and Jefferis, G. S. X. E. 2016. Genetically targeted 3D visualisation of *Drosophila*

- neurons under electron microscopy and X-ray microscopy using minisOG. Sci. Rep. 6:1-14.
- Oi, T., Enomoto, S., Nakao, T., Arai, S., Yamane, K., and Taniguchi, M. 2017. Three-dimensional intracellular structure of a whole rice mesophyll cell observed with FIB-SEM. Ann. Bot. 120:21-28.
- Okolo, C. A. 2022. A guide into the world of high-resolution 3D imaging: The case of soft X-ray tomography for the life sciences. Biochem. Soc. Trans. 50:649-663.
- Oreopoulos, J., Berman, R., and Browne, M. 2014. Spinning-disk confocal microscopy. Methods Cell Biol. 123:153-175.
- Otegui, M. S. 2020. Electron tomography and immunogold labeling of plant cells. Methods Cell Biol. 160:21-36.
- Ovec'ka, M., Sojka, J., Tichá, M., Komis, G., Basheer, J., Marchetti, C., Šamajová, O., Kube'nová, L., and Šamaj, J. 2022. Imaging plant cells and organs with light-sheet and super-resolution microscopy. Plant Physiol. 188:683-702.
- Pasternak, T., Tietz, O., Rapp, K., Begheldo, M., Nitschke, R., Ruperti, B., and Palme, K. 2015. Protocol: An improved and universal procedure for whole-mount immunolocalization in plants. Plant Methods 11:50.
- Pathan, A. K., Bond, J., and Gaskin, R. E. 2010. Sample preparation for SEM of plant surfaces. Mater. Today 12(Supp.1):32-43.
- Peddie, C. J., and Collinson, L. M. 2014. Exploring the third dimension: Volume electron microscopy comes of age. Micron 61:9-19.
- Pinedo, M., Canal, L., and Marcos Lousa, C. 2021. A call for rigor and standardization in plant extracellular vesicle research. J. Extracellular Vesicles 10:e12048.
- Proseus, T. E., and Boyer, J. S. 2005. Turgor pressure moves polysaccharides into growing cell walls of *Chara corallina*. Ann. Bot. 95:967-979.
- Rae, J., Ferguson, C., Ariotti, N., Webb, R. I., Cheng, H.-H., Mead, J. L., Riches, J. D., Hunter, D. J., Martel, N., Baltos, J., Christopoulos, A., Bryce, N. S., Cagigas, M. L., Fonseka, S., Sayre, M. E., Hardeman, E. C., Gunning, P. W., Gambin, Y., Hall, T. E., and Parton, R. G. 2021. A robust method for particulate detection of a genetic tag for 3D electron microscopy. eLife 10:e64630.
- Read, S. M., and Bacic, A. 1996. Cell wall porosity and its determination. Pages 63-80 in: Plant Cell Wall Analysis. Modern Methods of Plant Analysis, Vol. 17. H. F. Linskens, J. F. Jackson, eds. Springer, Berlin.
- Roth, R., Hillmer, S., Funaya, C., Chiapello, M., Schumacher, K., Lo Presti, L., Kahmann, R., and Paszkowski, U. 2019. Arbuscular cell invasion coincides with extracellular vesicles and membrane tubules. Nat. Plants 5:204-211.
- Rufián, J. S., Macho, A. P., Corry, D. S., Mansfield, J. W., Ruiz-Albert, J., Arnold, D. L., and Beuzón, C. R. 2018. Confocal microscopy reveals in planta dynamic interactions between pathogenic, avirulent and non-pathogenic *Pseudomonas syringae* strains. Mol. Plant Pathol. 19: 537-551.
- Rust, M. J., Bates, M., and Zhuang, X. 2006. Sub-diffraction-limit imaging by stochastic optical reconstruction microscopy (STORM). Nat. Methods 3:793-796.
- Rutter, B. D., and Innes, R. W. 2017. Extracellular vesicles isolated from the leaf apoplast carry stress-response proteins. Plant Physiol. 173:728-741.
- Salmén, F., Ståhl, P. L., Mollbrink, A., Navarro, J. F., Vickovic, S., Frisén, J., and Lundeberg, J. 2018. Barcoded solid-phase RNA capture for spatial transcriptomics profiling in mammalian tissue sections. Nat. Protoc. 13:2501-2534.
- Schaffer, M., Pfeffer, S., Mahamid, J., Kleindiek, S., Laugks, T., Albert, S., Engel, B. D., Rummel, A., Smith, A. J., Baumeister, W., and Plitzko, J. M. 2019. A cryo-FIB lift-out technique enables molecular-resolution cryo-ET within native *Caenorhabditis elegans* tissue. Nat. Methods 16: 757-762
- Schertel, A., Snaidero, N., Han, H.-M., Ruhwedel, T., Laue, M., Grabenbauer, M., and Möbius, W. 2013. Cryo FIB-SEM: Volume imaging of cellular ultrastructure in native frozen specimens. J. Struc. Biol. 184:355-360
- Schubert, V. 2017. Super-resolution microscopy applications in plant cell research. Front. Plant Sci. 8:1-12.
- Shu, X., Lev-Ram, V., Deerinck, T. J., Qi, Y., Ramko, E. B., Davidson, M. W., Jin, Y., Ellisman, M. H., and Tsien, R. Y. 2011. A genetically encoded tag for correlated light and electron microscopy of intact cells, tissues, and organisms. PLoS Biol. 9:e1001041.
- Sibarita, J.-B. 2005. Deconvolution microscopy. Pages 201-243 in: Microscopy Techniques. Advances in Biochemical Engineering, Vol. 95. J. Rietdorf, ed. Springer, Berlin.

- Smith, S. J. 2018. Q&A: Array tomography. BMC Biol. 16:98.
- Soukup, A., and Tylová, E. 2019. Essential methods of plant sample preparation for light microscopy. Pages 1-26 in: Plant Cell Morphogenesis. Methods in Molecular Biology, Vol. 1992. F. Cvrc ková and V. Žárský, eds. Humana, New York.
- Staedler, Y. M., Masson, D., and Schönenberger, J. 2013. Plant tissues in 3D via X-ray tomography: Simple contrasting methods allow high resolution imaging. PLoS One 8:e75295.
- Strock, C. F., Schneider, H. M., Galindo-Castañeda, T., Hall, B. T., Van Gansbeke, B., Mather, D. E., Roth, M. G., Chilvers, M. I., Guo, X., Brown, K., and Lynch, J. P. 2019. Laser ablation tomography for visualization of root colonization by edaphic organisms. J. Exp. Bot 70:5327-5342.
- Sydor, A. M., Czymmek, K. J., Puchner, E. M., and Mennella, V. 2015. Super-resolution microscopy: From single molecules to supramolecular assemblies. Trends Cell Biol. 25:730-748.
- Tamada, Y., Murata, T., Hattori, M., Oya, S., Hayano, Y., Kamei, Y., and Hasebe, M. 2014. Optical property analyses of plant cells for adaptive optics microscopy. Int. J. Optomechatronics 8:89-99.
- Tan, W. C. C., Nerurkar, S. N., Cai, H. Y., Ng, H. H. M., Wu, D., Wee, Y. T. F., Lim, J. C. T., Yeong, J., and Lim, T. K. H. 2020. Overview of multiplex immunohistochemistry/immunofluorescence techniques in the era of cancer immunotherapy. Cancer Commun. 40:135-153.
- Théroux-Rancourt, G., Roddy, A. B., Earles, J. M., Gilbert, M. E., Zwieniecki, M. A., Boyce, C. K., Tholen, D., McElrone, A. J., Simonin, K. A., and Brodersen, C. R. 2021. Maximum CO<sub>2</sub> diffusion inside leaves is limited by the scaling of cell size and genome size. P. R. Soc. B, 288:20203145
- Ursache, R., Andersen, T. G., Marhavý, P., and Geldner, N. 2018. A protocol for combining fluorescent proteins with histological stains for diverse cell wall components. Plant J. 93:399-412.
- van't Padje, A., Oyarte Galvez, L., Klein, M., Hink, M. A., Postma, M., Shimizu, T., and Kiers, E. T. 2021. Temporal tracking of quantum-dot apatite across in vitro mycorrhizal networks shows how host demand can influence fungal nutrient transfer strategies. ISME J. 15:435-449.
- Vidavsky, N., Akiva, A., Kaplan-Ashiri, I., Rechav, K., Addadi, L., Weiner, S., and Schertel, A. 2016.Cryo-FIB-SEM serial milling and block face imaging: Large volume structural analysis of biological tissues preserved close to their native state. J. Struc. Biol. 196:487-495.
- Villarraga-Gómez, H., Rad, M. N., Andrew, M., Andreyev, A., Sanapala, R., Omlor, L., and Graf vom Hagen, C. 2022. Improving throughput and image quality of high-resolution 3D X-ray microscopes using deep learning reconstruction techniques. 11th Conference on Industrial Computed Tomography (iCT) 2022, 8-11 Feb, Wels, Austria. eJNDT 27:3-8.
- Walker, N. C., White, S. M., McKay Fletcher, D., Ruiz, S. A., Rankin, K. E.,
  De Stradis, A., Saponari, M., Williams, K. A., Petroselli, C., and Roose,
  T. 2023. The impact of xylem geometry on olive cultivar resistance to
  Xylella fastidiosa: An image-based study. Plant Pathol. 72:521-535.
- Warner, C. A., Biedrzycki, M. L., Jacobs, S. S., Wisser, R. J., Caplan, J. L., and Sherrier, D. J. 2014. An optical clearing technique for plant tissues allowing deep imaging and compatible with fluorescence microscopy. Plant Physiol. 166:1684-1687.
- Weiner, E., Pinskey, J. M., Nicastro, D., and Otegui, M. S. 2022. Electron microscopy for imaging organelles in plants and algae. Plant Physiol. 188:713-725.
- Wightman, R. 2022. An overview of cryo-scanning electron microscopy techniques for plant imaging. Plants 11:1113.
- Wu, G.-H., Mitchell, P. G., Galaz-Montoya, J. G., Hecksel, C. W., Sontag, E. M., Gangadharan, V., Marshman, J., Mankus, D., Bisher, M. E., Lytton-Jean, A. K. R., Frydman, J., Czymmek, K., and Chiu, W. 2020. Multi-scale 3D cryo-correlative microscopy for vitrified cells. Structure 28:1231-1237.E3.
- Wu, Q., Luo, A., Zadrozny, T., Sylvester, A., and Jackson, D. 2013. Fluorescent protein marker lines in maize: Generation and applications. Int. J. Dev. Biol. 57:535-543.
- Wu, Y., and Shroff, H. 2018. Faster, sharper, and deeper: Structured illumination microscopy for biological imaging. Nat. Methods 15:1011-1019.
  Xia, C., Fan, J., Emanuel, G., Hao, J., and Zhuang, X. 2019. Spatial transcriptome profiling by MERFISH reveals subcellular RNA compartmentalization and cell cycle-dependent gene expression. Proc. Natl. Acad. Sci. U.S.A. 116:19490-19499.
- Young, C. L., Raden, D. L., Caplan, J. L., Czymmek, K. J., and Robinson, A. S. 2012. Cassette series designed for live-cell imaging of proteins and high-resolution techniques in yeast. Yeast 29:119-136.